Exploring the Biological and Theoretical Aspects of Rare Earth Metal Mixed Ligand Complexes: A Synergistic Approach

Synopsis Submitted in

Partial Fulfilment of the Requirements for the Degree of

Doctor of Philosophy

In

Chemistry

By

Jani Dharmilkumar Nileshbhai
220830340003

Under the Supervision of

Dr. Darshan H. Jani
Department of Chemistry
Associate Professor
School of Science
Dr. Subhash University

Dr. Subhash University
Dr. Subhash Road, Junagadh – 362001, Gujarat, India.

December 2025

CERTIFICATE OF ORIGINALITY

It is certified that Ph.D. Thesis titled "**Exploring the Biological and Theoretical Aspects of Rare Earth Metal Mixed Ligand Complexes: A Synergistic Approach**" by **Dharmilkumar Nileshbhai Jani** has been examined by me/us.

I/We undertake the following:

A. Thesis has significant new work/knowledge as compared already published or are under consideration to be published elsewhere. No sentence, equation, diagram, table, paragraph or section has been copied verbatim from previous work unless it is placed under quotation marks and duly referenced.
B. The work presented is original and own work of the author (i.e. there is no plagiarism), No ideas, processes, results or words of others have been presented as Author own work.
C. There is no fabrication of data or results which have been compiled / analyzed.
D. There is no falsification by manipulating research materials, equipment or processes, or changing or omitting data or results such that the research is not accurately represented in the research record.
E. The thesis has been checked using Drillbit Software (copy of originality report attached) and found within limits as per Dr. Subhash Univeristy (DSU) Plagiarism Policy and instructions issued from time to time (i.e. permitted similarity index ≤10%).

Signature of Research scholar: 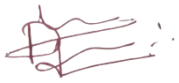 Date: 09-12-2025

Name of the Research scholar: Dharmilkumar Nileshbhai Jani

Name & Signature of Supervisor

Dr. Darshan H. Jani
Asso. Professor,
Department of Chemistry,
School of Science,
Dr. Subhash University – Junagadh.

CERTIFICATE

This is to certify that the thesis entitled **"Exploring the Biological and Theoretical Aspects of Rare Earth Metal Mixed Ligand Complexes: A Synergistic Approach"** is a bonafide record of research work carried out by **Dharmilkumar Nileshbhai Jani** (220830340003), Research Scholar, Department of Centre for Research and Development, School of Science, Dr. Subhash University - Junagadh, under my/our supervision/guidance during the period *August 2022 – December 2025*. To the best of our knowledge: (I) the candidate has not submitted the same research work to any other University or Institute for any Degree, Diploma, Associateship, Fellowship or other similar titles (II) the thesis submitted is a record of original research work done by the Research scholar during the period of study under our supervision, and (III) the thesis represents independent research work on the part of the Research scholar.

Place: Junagadh

Date: 09-12-2025

Name & Signature of Supervisor

Dr. Darshan H. Jani
Asso. Professor,
Department of Chemistry,
School of Science,
Dr. Subhash University – Junagadh.

DECLARATION

I, **Dharmilkumar Nileshbhai Jani**, Research scholar in the Department of Centre for Research and Development, declare that the work embodied in the Ph.D. thesis entitled, **"Exploring the Biological and Theoretical Aspects of Rare Earth Metal Mixed Ligand Complexes: A Synergistic Approach"** is my original and bonafide work carried out by me under the supervision of **Dr. Darshan H. Jani**, Asso. Professor, Dr. Subhash University for a period from *August 2022* to *December 2025* at Dr. Subhash University.

I further declare that the contents embodied in this thesis have not been submitted for the award of any degree, diploma, associateship, fellowship or other similar title to any other University or Institute.

I confirm that I have duly acknowledged and given credit to the work of other researchers wherever cited in the text, tables, figures and the body of the thesis. I also declare that I have not will fully copied or reproduced others' work, data, results, etc., as reported in journals, books, magazines, reports, dissertations, theses, or available on websites, and claimed it as my own.

I shall be solely responsible for the **originality of the entire content** and any **plagiarism** found in the thesis.

Place: Junagadh

Date:09-12-2025

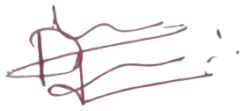

Dharmilkumar Nileshbhai Jani

Enrol. No.: **220830340003**

Table of Contents

List of Tables vi

List of Figures vii

Abstract viii

Graphical Abstract ix

Chapter 1 1

1.1. Introduction & Review of Literature of Biological activity of Schiff base and it's Heterochelates 1

1.2. Synthetic aspect of Schiff base as ligands 5

1.3. Objectives of Study 5

Chapter 2 7

2.1. Materials & Finding Techniques 7

2.2. Methods 7

2.2.1. Common Process for Ligand Synthesis 7

2.2.2. Common Process for Heterochelate synthesis 8

2.2.3. Common process for acylation 8

Chapter 3 9

3.1. Analytical and Physical characteristics of ligands and it's Heterochelates 9

3.2. Results and Discussion 11

3.2.1. ^{1}H-NMR 12

3.2.2. IR 12

3.2.3. UV 12

3.2.4. FAB Mass 13

Chapter 4 14

4.1. Analytical and Physical characteristics of ligands and it's Heterochelates 14

4.2. Results and Discussion 15

4.2.1. ^{1}H-NMR 15

4.2.2. IR 15

4.2.3. UV 16

4.2.4. FAB Mass 17

Chapter 5 18

5.1. Anti-Microbial and Anti-Fungal Activities 18

5.2. Computational Analysis of Ligands 19
5.3. Molecular Docking study of Ligands 19
5.4. Conclusion 19
Publications 21
Reference 22

List of Tables

Table 3.1 Analytical and Physical data of Ligands and Heterochelates.....9

Table 4.1 Analytical and Physical data of Ligands and Heterochelates.....14

List of Figures

Figure 1.1 Proposed Structure of chromium (III) complex 2
Figure 1.2 Proposed structure of uranyl (VI) complex 3
Figure 1.3 Proposed structure of Cu(II) complex and Ligand 4
Figure 1.4 Proposed structure of Cu(II)-Gd(III) SB Complex 4
Figure 1.5 Schiff base and its heterochelate: a general synthesis 5
Figure 3.1 Suggested fragmentation pattern of heterochelate $[(L_1)_2ZrO]$ 13
Figure 4.1 Suggested fragmentation pattern of heterochelate $[(L_8)_2ZrO]$ 17
Figure 5.1 Zone of inhibition in mm (a) $[(L_1)_2VO]$ E. Coli (b) $[(L_1)_2WO_2]$
E. Coli (c) $[(L_1)_2VO]$ S. aureus (d) $[(L_1)_2WO_2]$ S. aureus 18

.

Exploring the Biological and Theoretical Aspects of Rare Earth Metal Mixed Ligand Complexes: A Synergistic Approach

Abstract

In this work, a novel bidentate Schiff base ligand synthesized by using 4-Amino-N-(6-methoxypyrimidine-4-yl)benzenesulfonamide further used to synthesize and characterize a series of metal complexes of molybdenum (Mo), tungsten (W), vanadium (V), and zirconium (Zr). Mass spectrometry, UV-visible, FT-IR, ^{1}H-NMR spectroscopy, and elemental analysis were used to synthesize and analyse the ligand and its associated metal complexes. Gram-positive bacteria *S. aureus, B. subtilis*, Gram-negative bacteria *E. coli, P. aeruginosa*, and the fungal strain *A. niger* were used to test the synthetic compound's antibacterial and antifungal properties. The findings showed that, in contrast to the free ligand, the metal complexes had higher biological activity. Positive interactions between the synthesized complexes and pertinent biomolecular targets were further validated by molecular docking experiments, suggesting that they have the potential to be promising bioactive agent. The overall findings highlight the significance of transition metal coordination chemistry in the development of novel antimicrobial candidates and provide a basis for future exploration in this field.

Graphical Abstract

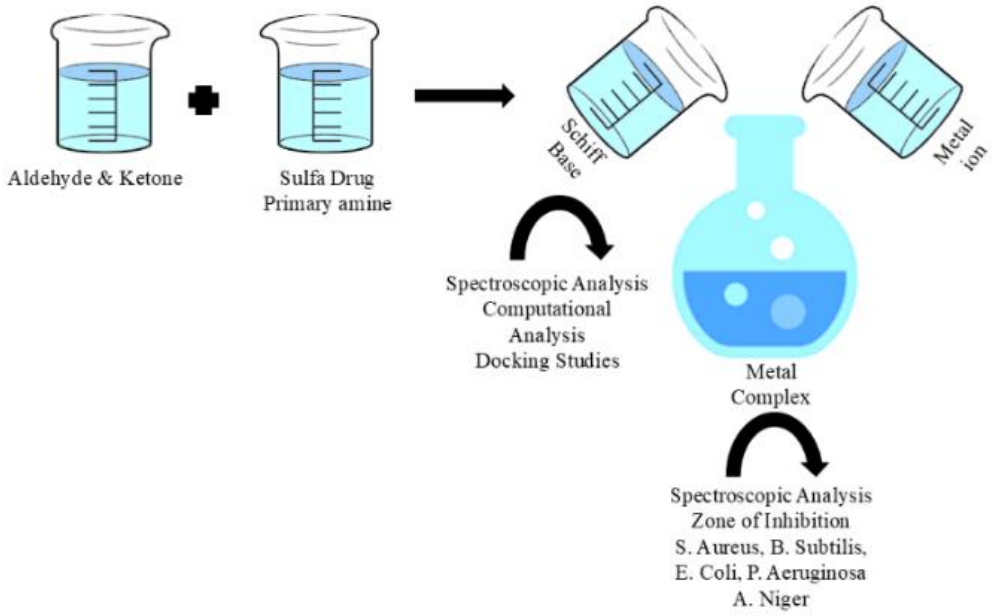

Chapter 1
Introduction, Literature review & Objectives

1.1. Introduction & Review of Literature of Biological activity of Schiff base and it's Heterochelates

Globally, microbial antibiotic resistance has emerged as a major concern. The generation of unprecedented anti-infective therapeutic entities can be effectuated through the strategic re-exploitation of pharmacological agents whose clinical trajectories have been recently discontinued, in conjunction with the deliberate morphological transfiguration of their underlying bioactive molecular scaffolds. Synthetic antimicrobial compounds known as sulphonamides, or sulfa medications, are used to treat illnesses caused by bacteria, certain fungi, and protozoa. They were the first class of extensively used antibacterials and a time in the history of antibiotics.[1] The extraordinary pharmacodynamic propensities exhibited by transition metal coordinated schiff base architectures originating from sulfonamide based therapeutic agents have been subjected to exhaustive and multifaceted scientific interrogation across an extensive span of medicinal chemical investigation.[2-5] Organic molecules with π-conjugated systems are highly versatile, allowing for a variety of substitutions and functions, making them important in organometallic chemistry and biochemistry.[6,7] Schiff base frameworks have achieved pervasive applicability across a vast constellation of chemical enterprises including, but not confined to, advanced synthetic methodologies, multifarious coordination-chemical paradigms, and an array of biologically operative systems where they function as indispensable molecular protagonists.[10]

Among the most monumental and paradigm defining bequests that coordination chemistry has imparted to the domain of medicinal chemistry is the serendipitous elucidation of cisplatin formally designated as cis-diammine-dichloroplatinum(II) together with its structurally modulated congeners, whose prodigious cytotoxic proclivities have manifested as exceptionally potent anticancer pharmacophores. In order to close the gap between inorganic and medicinal chemistry, this has spurred interest in developing new molecules based on metals with biological activity.[11] Platinum and ruthenium centred coordination entities constitute some of the most ubiquitously

deployed metallotherapeutic constructs in contemporary oncological intervention, whereas complexes incorporating radio nuclidic ^{99m}Tc and paramagnetic Gd^{3+} utilized respectively within the sophisticated diagnostic architectures of scintigraphic imaging and magnetic-resonance modalities represent additional exemplars of exceptionally efficacious metal-based biomedical agents.

One of the earliest medicinal Metallo-Pharmaceuticals used to treat syphilis was Salvarsan, an arsenic-based antibacterial agent developed by Paul Ehrlich. From its discovery at the beginning of the 20th century until penicillin replaced it following World War II, it was in use. Yet another highly illustrative paradigm is furnished by argentous coordination assemblies employed with notable frequency in anti-infective therapeutics, together with sulfonamide based topical preparations exemplified by silver sulfadiazine which are administered in cream-like matrices or as aqueous dispersions containing approximately one percent argentous salt, for the prophylaxis and remediation of pathogenic complications arising from cutaneous trauma of second or third degree severity.[12]

The trivalent transition metal tetraaza macrocyclic complexes were created by Rathi et al. using 5,5-dimethylcyclohexane-1,3-dione and 1,8-diaminonaphthalene. Their investigative assessments meticulously delineated the multifarious antibacterial and antioxidative proficiencies embedded within the resultant coordination constructs. Within this assemblage, the molecular entity designated as Complex 1 emerged as exhibiting the most pronounced and preeminent bio functional potency across both antimicrobial and radical quenching paradigms. Consequently, this particular molecular archetype may be construed as an exceptionally propitious foundational scaffold from which the rational design and progressive development of future pharmacotherapeutic entities could be systematically initiated.[13]

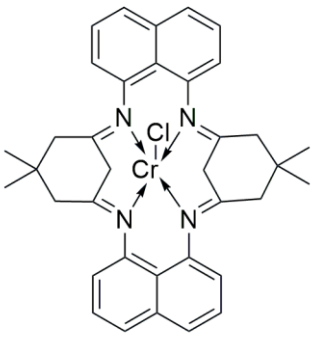

Complex 1

Figure 1.1 Proposed Structure of chromium (III) complex

According to De Oliveira et al., research utilizing uranyl(VI) complexes (Complex 2) with Salen type Schiff bases has demonstrated their remarkable potential as effective electrochemical modifiers for cocaine detection. These compounds showed exceptional sensitivity and selectivity toward cocaine when used to modify various electrodes, such as platinum, glassy carbon, and screen-printed electrodes, even in the presence of common interfering substances including lidocaine, procaine, morphine, and MDMA. The findings demonstrate that the $[UO_2(3\text{-MeO-salen})(H_2O)]\cdot H_2O$ complex in particular offers consistent and interference free voltametric responses, making these modified electrodes perfect tools for rapid, inexpensive, and accurate preliminary forensic investigation of cocaine in confiscated drug samples.[14]

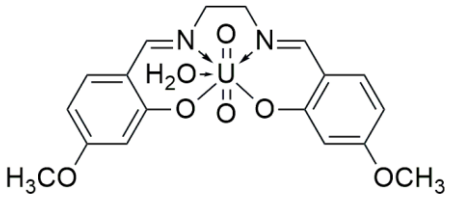

Complex 2

Figure 1.2 Proposed structure of uranyl (VI) complex

Quinolin-2(1H)-one was used to create Schiff bases (1) and their Cu(II) complex (Complex 3). The mycocidal and cytotoxic propensities inherent to the synthesized molecular entities were subjected to in-vitro interrogation within rigorously controlled bioanalytical frameworks. The human hepatic carcinoma cell line Hep-G2 was used to assess anticancer potential. Cisplatin was used as the standard drug for the comparison. The 7-(2-hydroxybenzylideneamino-3-ethoxy)-based Cu(II) coordination architectures derived from Schiff-base ligation exhibit conspicuous pharmacological promise, a conclusion substantiated by the pronounced cytotoxic disposition displayed by the associated 4-methylquinolin-2(1H)-one moiety, which functions as a pivotal bioactive determinant within the system.[15]

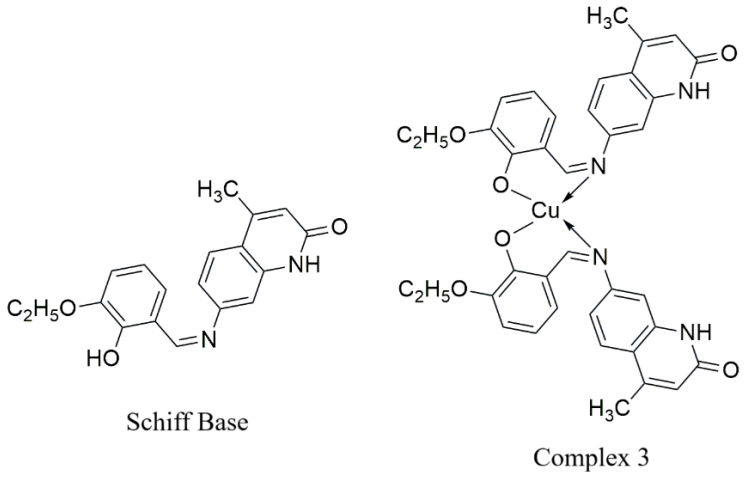

Figure 1.3. Proposed structure of Cu(II) complex and Ligand

Keshavarzian et al. published a study on a dimetallic compound including copper (II) and gadolinium (III) in 2022. After examining the Cu(II)-Gd(III) SB complex (Complex 4) for its binding affinity with FS-DNA using a range of analytical techniques, intercalation was suggested as the main pathway of binding. The associative engagement of the complexes with bovine serum albumin (BSA) manifested a markedly substantive degree of biomolecular complexation, the intricacies of which were subjected to subsequent analytical elucidation through multifaceted spectrochemical interrogation. The MTT assay showed antiproliferative activity against the cancer cell lines MCF-7, HeLa, and human prostate cancer (LNCaP). The catalytic activity and mechanism of the complex in the 3,5-di-tert-butylcatechol oxidation process were eventually investigated at 298 K. The chemical exhibited a moderate degree of catecholase activity in DMF medium.[16]

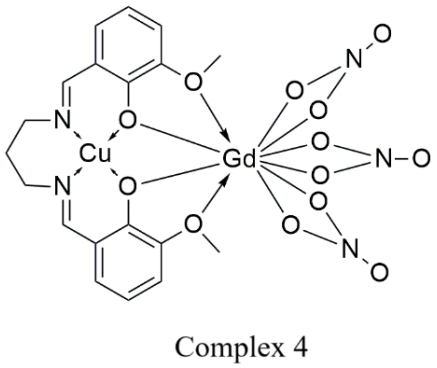

Figure 1.4 Proposed structure of Cu(II)-Gd(III) SB Complex

1.2. Synthetic aspect of Schiff base as ligands

A nucleophilic addition-elimination process yields a Schiff base. An intermediate molecule is produced when the amine attacks the carbonyl carbon nucleophilic way. After that, a water molecule is eliminated to create the final Schiff base. It warrants particular emphasis that Schiff-base assemblages frequently persist in a dynamic, solution-phase equilibria interplay with their progenitor carbonyl substrates and amine counterparts, thereby constituting a continuously fluctuating molecular speciation regime. They can hydrolyse under specific circumstances, breaking the carbon-nitrogen double bond and returning to the original amine and carbonyl molecules. The general structure of Schiff base can be represented as

R_1-C=N-R_2

In this formula,

R_1 represents the organic group attached to the carbon atom.

C stands for the carbon atom in the aldehyde or ketone's carbonyl group.

N represents the nitrogen atom, which forms the double bond with the carbon atom.

R2 stands for an organic group that is joined to the amine group's nitrogen atom

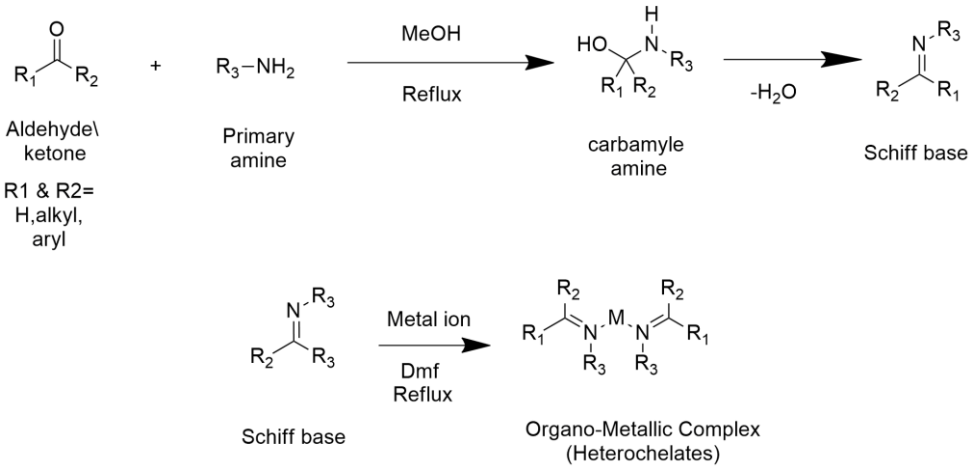

Figure 1.5 Schiff base and its heterochelate: a general synthesis

1.3. Objectives of Study

This study's primary goal is to create and describe Schiff base ligand heterochelates and investigate their unique coordination behaviour and structural diversity. The study looks at the effects of various metal ions on the formation and stability of these complexes, taking into account both steric and electronic factors. Their structures will be clarified using several analytical and spectroscopic

techniques, including FT-IR, UV-Vis, ^{1}H-NMR, and mass spectrometry. The electronic and structural features of the ligands will also be analysed through DFT calculations, with a particular focus on the HOMO–LUMO energy gap. Molecular docking studies will further be carried out to investigate how the ligands interact with selected biological macromolecules and to assess their binding affinity. In addition, the biological potential of the synthesized compounds will be evaluated to understand their antimicrobial and antifungal effectiveness. By systematically modifying the Schiff base ligands, this work aims to improve ligand-design strategies and deepen the understanding of structure–activity relationships. All things considered, the research advances the subject of coordination chemistry and aids in the creation of novel functional materials with potential uses in both science and industry.

Chapter 2

Materials & Methods

2.1. Materials & Finding Techniques

The starting materials, reagents, and solvents utilized in the tests were all quite pure, bought from a local provider, and employed immediately without further purification. Using Merck pre-coated aluminium sheets and 60 F-254 silica gel plates, the reaction's development was assessed using thin-layer chromatography (TLC). The mobile phase was an optimized solvent system, and iodine vapor and UV light were utilized to visualize the results.

While ^{1}H-NMR spectra were recorded in DMSO-d6 solution using an AvanceNeo Ascend 400 MHz instrument at a nearby research institution, A Perkin-Elmer spectrometer operating in the 4000–400 cm^{-1} range was used to acquire infrared (IR) spectra. KBr pellet method using a Nicolet-400D spectrophotometer was also used to measure FT-IR spectra. The UV-Vis spectrophotometer V-750 was used to gather UV spectra.

2.2. Methods

2.2.1. Common Process for Ligand Synthesis

The synthesis of all the ligand was achieved by reacting 10 mmol of 4-Amino-N-(6-methoxypyrimidine-4-yl)benzenesulfonamide with an equimolar number of different derivatives of 2-hydroxybenzaldehyde/ 4-acylpyrazolone in methanol under continuous stirring at 35°C. Using a hexane/ethyl acetate (7:3) combination as the mobile phase, thin-layer chromatography (TLC) was used to track the reaction's progress and verify that all of the starting ingredients had been consumed within 30 minutes. After everything was finished, the solid product was separated by filtering, completely cleaned with ethanol, dried at 60°C, and then stored for later use.

2.2.2. Common Process for Heterochelate synthesis

All heterochelates were synthesised and isolated using a general method. With constant stirring and drop by drop addition of warm metal salt solution prepared in DMF was added to the respective ligand solution in 1:2 Metal to Ligand molar ratios. The mixture was heated for four hours at 70˚C and then allowed to cool overnight at room temperature. A densely coloured product emerged after cooling to ambient temperature and was then let it for drying in desiccators.

2.2.3. Common process for acylation

15 gm of 1-phenyl-3-methyl-pyrazolone were placed in a flask equipped with a stirrer, separatory funnel and a reflux condenser and dissolved in 60-80 ml dioxane by application of heat. After adding 12g of calcium hydroxide, 0.056 mol of acyl chloride was added dropwise over the course of one minute. Over the first several minutes, the temperature rose and the reaction mixture turned into a thick paste. The mixture was heated for thirty minutes to cause reflux. Buff-coloured crystals separated when the mixture was added to diluted hydrochloric acid (200 ml, 2N), which broke down the calcium complex in the flask. The crystals were collected on Buchner funnel. They were recrystallized from methanol-water slightly acidified to destroy any decomposed calcium complex.

Chapter 3

Physical properties, Spectroscopic data & Characterization of Ligands and Heterochelates– I

3.1. Analytical and Physical characteristics of ligands and it's Heterochelates

Table 3.1 Analytical and Physical data of Ligands and Heterochelates

Compound	M.Wt	Colour & % Yeild	Analysis (%) Found (cal)			
			C	H	N	M
L_1 $C_{18}H_{16}N_4O_4S$	384.09	Yellow 81%	56.22 (56.24)	4.19 (4.20)	14.55 (14.57)	-
$[(L_1)_2MoO_2]$ $C_{36}H_{30}N_8O_{10}S_2Mo$	894.76	Orange 79%	48.27 (48.32)	3.34 (3.38)	12.48 (12.52)	10.78 (10.72)
$[(L_1)_2WO_2]$ $C_{36}H_{30}N_8O_{10}S_2W$	982.64	Brown 81%	43.97 (44.00)	3.04 (3.08)	11.37 (11.40)	18.79 (18.71)
$[(L_1)_2VO]$ $C_{36}H_{30}N_8O_9S_2V$	833.74	Green 83%	51.83 (51.86)	3.59 (3.63)	13.37 (13.44)	6.17 (6.11)
$[(L_1)_2ZrO]$ $C_{36}H_{30}N_8O_9S_2Zr$	874.03	Yellow 77%	49.44 (49.47)	3.44 (3.46)	12.80 (12.82)	14.51 (14.44)
L_2 $C_{19}H_{18}N_4O_5S$	414.44	Orange 79%	55.04 (55.06)	4.36 (4.38)	13.51 (13.52)	-
$[(L_2)_2MoO_2]$ $C_{38}H_{34}N_8O_{12}S_2Mo$	954.81	Red 78%	47.76 (47.80)	3.57 (3.59)	11.69 (11.74)	10.11 (10.05)
$[(L_2)_2WO_2]$ $C_{38}H_{34}N_8O_{12}S_2W$	1042.69	Brown 73%	43.73 (43.77)	3.27 (3.29)	10.71 (10.75)	17.69 (17.63)

$[(L_2)_2VO]$ $C_{38}H_{34}N_8O_{11}S_2V$	893.80	Buff 86%	51.01 (51.06)	3.80 (3.83)	12.51 (12.54)	5.77 (5.70)
$[(L_2)_2ZrO]$ $C_{38}H_{34}N_8O_{11}S_2Zr$	934.08	Red 81%	48.82 (48.86)	3.63 (3.67)	12.96 (12.00)	9.81 (9.77)
L_3 $C_{18}H_{15}N_5O_6S$	429.41	Orange 74%	50.32 (50.35)	3.52 (3.52)	16.28 (16.31)	-
$[(L_3)_2MoO_2]$ $C_{36}H_{28}MoN_{10}O_{14}S_2$	984.76	Brown 74%	43.88 (43.91)	2.85 (2.87)	14.20 (14.22)	9.81 (9.74)
$[(L_3)_2WO_2]$ $C_{36}H_{28}N_{10}O_{14}S_2W$	1072.64	Brown 73%	40.29 40.31	2.59 (2.63)	13.04 (13.06)	17.19 (17.14)
$[(L_3)_2VO]$ $C_{36}H_{28}N_{10}O_{13}S_2V$	923.74	Black 87%	46.77 (46.81)	3.02 (3.06)	15.13 (15.16)	5.54 (5.51)
$[(L_3)_2ZrO]$ $C_{36}N_{28}N_{10}O_{13}S_2Zr$	964.02	Brown 79%	44.83 (44.85)	2.89 (2.93)	14.51 (14.53)	9.51 (9.46)
L_4 $C_{22}H_{25}N_5O_4S$	455.53	Yellow 89%	57.99 (58.01)	5.51 (5.53)	15.35 (15.37)	-
$[(L_4)_2MoO_2]$ $C_{44}H_{48}MoN_{10}O_{10}S_2$	1037	Brown 73%	50.92 (50.96)	4.64 (4.67)	13.49 (13.51)	9.31 (9.25)
$[(L_4)_2WO_2]$ $C_{44}H_{48}N_{10}O_{10}S_2W$	1124.88	Dark Brown 78%	46.45 (46.98)	4.28 (4.30)	12.43 (12.45)	16.37 (16.34)
$[(L_4)_2VO]$ $C_{44}H_{48}N_{10}O_9S_2V$	975.99	Brown 87%	54.13 (54.15)	4.93 (4.96)	14.31 (14.35)	5.29 (5.22)
$[(L_4)_2ZrO]$ $C_{44}H_{48}N_{10}O_9S_2Zr$	1016.27	Brown 79%	51.97 (52.00)	4.73 (4.76)	13.75 (13.78)	9.01 (8.98)
L_5 $C_{17}H_{16}N_4O_4S_2$	372.40	Buff 89%	54.81 (54.83)	4.31 (4.33)	15.01 (15.04)	
$[(L_5)_2MoO_2(NH_4)_2]$ $C_{34}H_{40}MoN_{10}O_{10}S_2$	908.83	Orange 72%	44.91 (44.93)	4.42 (4.44)	15.39 (15.41)	10.61 (10.56)
$[(L_5)_2WO_2(Na)_2]$ $C_{34}H_{32}N_8Na_2O_{10}S_2W$	1006.61	Brown 77%	40.53 (40.57)	3.18 (3.20)	11.10 (11.13)	18.31 (18.26)
$[(L_5)_2VOSO_4]$ $C_{34}H_{32}N_8O_{13}S_3$	907.80	Brown 84%	45.02 (44.98)	3.52 (3.55)	12.31 (12.34)	5.65 (5.61)

$[(L_5)_2ZrO(NO_3)_2]$ $C_{34}H_{32}N_{10}O_{15}S_2Zr$	976. 003	Brown 73%	41.82 (41.84)	3.27 (3.30)	14.31 (14.35)	9.39 (9.35)
L_6 $C_{17}H_{16}N_4O_4S_2$	463.31	Orange 89%	46.64 (46.66)	3.22 (3.26)	12.07 (12.09)	-
$[(L_6)_2MoO_2]$ $C_{36}H_{28}Br_2MoN_8O_{10}S_2$	894.76	Orange 79%	48.27 (48.32)	3.34 (3.38)	12.48 (12.52)	10.78 (10.72)
$[(L_6)_2WO_2]$ $C_{36}H_{28}Br_2N_8O_{10}S_2W$	982.64	Brown 81%	43.97 (44.00)	3.04 (3.08)	11.37(11 .40)	18.79 (18.71)
$[(L_6)_2VO]$ $C_{36}H_{30}N_8O_9S_2V$	833.74	Green 83%	51.83 (51.86)	3.59 (3.63)	13.37(13 .44)	6.17 (6.11)
$[(L_6)_2ZrO]$ $C_{36}H_{30}N_8O_9S_2Zr$	874.03	Yellow 77%	49.44 (49.47)	3.44 (3.46)	12.80 (12.82)	14.51 (14.44)
L_7 $C_{25}H_{23}N_5O_6S_2$	553.61	Pink	54.21 (54.24)	4.17 (4.19)	12.62 (12.65)	-
$[(L_7)_2MoO_2]$ $C_{38}H_{34}N_8O_{12}S_2Mo$	954.81	Red 78%	47.76 (47.80)	3.57 (3.59)	11.69 (11.74)	10.11 (10.05)
$[(L_7)_2WO_2]$ $C_{38}H_{34}N_8O_{12}S_2W$	1042.69	Brown 73%	43.73(43. 77)	3.27 (3.29)	10.71 (10.75)	17.69 (17.63)
$[(L_7)_2VO]$ $C_{38}H_{34}N_8O_{11}S_2V$	893.80	Buff 86%	51.01(51. 06)	3.80 (3.83)	12.51 (12.54)	5.77 (5.70)
$[(L_7)_2ZrO]$ $C_{38}H_{34}N_8O_{11}S_2Zr$	934.08	Red 81%	48.82 (48.86)	3.63 (3.67)	12.96 (12.00)	9.81 (9.77)

3.2. Results and Discussion

The structure of synthesized ligands and their heterochelates was ascertained by elemental analysis, mass spectrometry, ^{1}H-NMR, FT-IR, UV, and FAB-Mass analytical and spectroscopic techniques. The experimental portion includes FAB-Mass on a heterochelate, UV of ligands and their heterochelates, ^{1}H-NMR, FT-IR, and elemental analysis. In DMF and DMSO, all of the compounds were fairly soluble and stable at ambient temperature.

3.2.1. ^{1}H-NMR

The experimental section presents the results of recording the ^{1}H NMR spectra of produced compounds in DMSO-d6 at room temperature. The –OCH_3 group appeared at 3.82–3.85 δ ppm in all ligands except L_5, with an additional –OCH_3 peak in L_2. The –OH signal was observed at 5.94–6.37 δ ppm (L_1–L_4) except for L_5. In L_4, peaks at 1.11 and 3.40 δ ppm correspond to –CH_3 and –CH_2 groups, respectively. Aromatic protons appeared as multiplets in the 6.38–9.06 δ ppm range. In L_7, the –CH_3 proton as a singlet at 1.27 δ ppm. A triplet–quartet pattern confirms the presence of the –OCH_2CH_3 group. Overlapping –NH signals made individual assignments difficult, but proton counts matched the molecular formulas, further supported by mass spectral data.

3.2.2. IR

To determine which groups are participate in metal coordination, the complexes infrared spectra were compared to those of the Schiff base ligand. The Schiff base ligand contains five potential donor sites: i) phenolic oxygen, ii) azomethine nitrogen, iii) sulfonamide nitrogen, iv) sulfonamide oxygen while ligand L_5 does not have phenolic -OH but contain oxygen of furan ring for chelation. The free ligands show a clear azomethine (C=N) band at 1570–1597 cm^{-1}, which shifts to a lower range around 1517–1570 cm^{-1} indicates that the azomethine nitrogen binds to the metal. In the complexes, the phenolic O–H band observed at 3238–3360 cm^{-1} in the free ligands vanishes, indicating deprotonation and coordination via oxygen. In contrast, the S=O band found at the range of 1134–1159 cm^{-1} which remains unchanged, showing that the sulfonyl group is not involved in binding. New bands in the 464–600 cm^{-1} and 601–700 cm^{-1} regions correspond to M–O and M–N vibrations, confirming metal oxygen and metal nitrogen coordination. Overall, the infrared data make it abundantly evident that the ligands function as bidentate donors, binding to the metal via the azomethine nitrogen and deprotonated oxygen atoms to create stable complexes.

3.2.3. UV

The ligands showed clear absorption bands between 250–350 nm, which correspond to the π→π* and n→π* transitions of the azomethine and aromatic groups. When the ligands formed complexes with metal ions, these bands shifted noticeably, indicating interactions involving the conjugated system and the lone pair on the azomethine nitrogen. Changes in peak position and intensity further suggest metal–ligand charge transfer and coordination effects. In the V(IV) complexes, additional bands appearing at 400–490 nm are attributed to d–d transitions. Their magnetic moment values found in the range of 1.69 - 1.73 B.M. which aligns with the presence of a single unpaired electron, confirming a low-spin d^1 configuration and their paramagnetic behaviour. Overall, magnetic data

and spectrum changes between the ligands and their metal complexes demonstrate effective coordination and bolster the synthetic compounds' structural stability.

3.2.4. FAB Mass

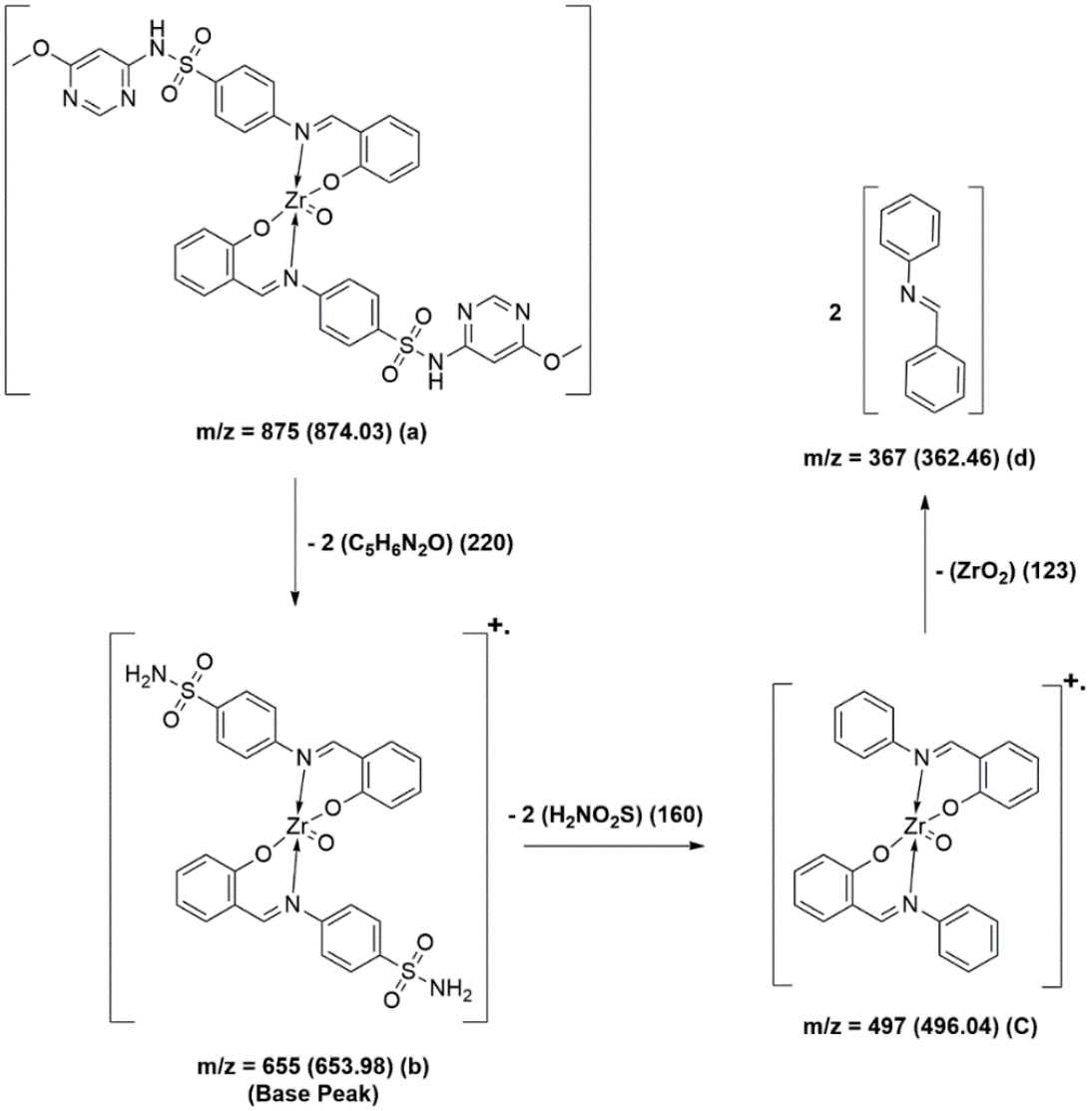

Figure 3.1 Suggested fragmentation pattern of heterochelate $[(L_1)_2ZrO]$

Chapter 4

Physical properties, Spectroscopic data & Characterization of Ligands and Heterochelates – II

4.1. Analytical and Physical characteristics of ligands and it's Heterochelates

Table 4.1 Analytical and Physical data of Ligands and Heterochelates

Compound	M.Wt.	Colour & % Yield	Analysis (%) Found (cal)			
			C	H	N	M
L_8 $C_{24}H_{24}N_6O_4S$	492.55	Buff 87%	58.50 (58.52)	4.87 (4.87)	17.04 (17.06)	-
$[(L_8)_2MoO_2]$ $C_{48}H_{46}N_{12}O_{10}S_2Mo$	1111.04	81% Brown	51.85 (51.89)	4.14 (4.17)	14.38 (14.40)	8.67 (8.64)
$[(L_8)_2WO_2]$ $C_{48}H_{46}N_{12}O_{10}S_2W$	1198.92	84% Red	48.07 (48.09)	3.83 (3.87)	13.99 (14.02)	15.37 (15.33)
$[(L_8)_2VO]$ $C_{48}H_{46}N_{12}O_9S_2V$	1050.03	71% Red	54.88 (54.90)	4.38 (4.42)	15.99 (16.01)	4.87 (4.85)
$[(L_8)_2ZrO]$ $C_{48}H_{46}N_{12}O_9S_2Zr$	1090.31	80% Brown	52.87 (52.88)	4.23 (4.25)	15.39 (15.42)	8.39 (8.37)
L_9 $C_{28}H_{24}N_6O_4S$	540.59	Buff 84%	62.19 (62.21)	4.43 (4.47)	15.52 (15.55)	-
$[(L_9)_2MoO_2]$ $C_{56}H_{46}N_{12}O_{10}S_2Mo$	1139.10	71% Brown	55.67 (55.72)	3.82 (3.84)	13.90 (13.92)	7.98 (7.95)

$[(L_9)_2WO_2]$ $C_{56}H_{46}N_{12}O_{10}S_2W$	1226.98	79% Red	51.92 (51.94)	3.54 (3.58)	12.94 (12.98)	14.22 (14.20)
$[(L_9)_2VO]$ $C_{56}H_{46}N_{12}O_9S_2V$	1078.08	84% Red	58.67 (58.69)	4.02 (4.05)	14.64 (14.67)	4.47 (4.44)
$[(L_9)_2ZrO]$ $C_{56}H_{46}N_{12}O_9S_2V$	1118.36	70% Brown	58.67 (58.69)	3.89 (3.91)	14.13 (14.17)	7.71 (7.69)

4.2. Results and Discussion

The structure of synthesized ligands and their heterochelates was ascertained by elemental analysis, mass spectrometry, ^{1}H-NMR, FT-IR, UV, and FAB-Mass analytical and spectroscopic techniques. The experimental portion includes FAB-Mass on a heterochelate, UV of ligands and their heterochelates, ^{1}H-NMR, FT-IR, and elemental analysis. In DMF and DMSO, all of the compounds were fairly soluble and stable at ambient temperature.

4.2.1. ^{1}H-NMR

The experimental section presents the results of recording the ^{1}H NMR spectra of produced compounds in DMSO-d6 at room temperature. The $–OCH_3$ group appeared at 3.85 δ ppm in both of the ligands. Other than that, there are peaks in ligand L_8 at 0.8 δ ppm & 1.5 δ ppm corresponding to $-CH_3$ & $-CH_2$ respectively also a common CH_3 peak is found which is common for both the ligands. Aromatic protons appeared as multiplets in the 6.38–8.45 δ ppm range. Overlapping –NH signals made individual assignments difficult, but proton counts matched the molecular formulas, further supported by mass spectral data.

4.2.2. IR

To determine which groups are participate in metal coordination, the complexes infrared spectra were compared to those of the Schiff base ligand. The ligand contains five potential donor sites: i) Pyrazolone oxygen, ii) azomethine nitrogen, iii) sulfonamide nitrogen, iv) sulfonamide oxygen. The IR spectra of the free ligands and their metal complexes were examined in order to ascertain the binding mode of rare earth transition metal complexes with Schiff base ligands. The azomethine ν(C=N) band appeared at 1653 cm^{-1} in L_8 and 1622 cm^{-1} in L_9, shifting to 1570–1595 cm^{-1} in the coordination compounds, indicating coordination through the azomethine nitrogen. New bond

observed at the range of 470 cm^{-1} to 586 cm^{-1} indicating M-O bond. The $\nu(SO_2)$ band was observed at 1163 cm^{-1} in L_8 and 1141 cm^{-1} in L_9 and 1188–1132 cm^{-1} in the heterochelates, which depicts confirming metal–ligand complex formation.

4.2.3. UV

The ligands displayed characteristic $\pi \rightarrow \pi^*$ transition bands in the 260–310 nm range, corresponding to the π-electron excitation within the aromatic and azomethine chromophores. These absorbance maxima showed discernible alterations upon complexation with metal ions, suggesting coordination of the ligands to the metal centres through donor sites such azomethine nitrogen and aromatic ring. The occurrence of ligand-to-metal charge transfer (LMCT) bands in the 270–350 nm region for several complexes confirms effective orbital overlap and charge transfer from ligand to metal, validating successful complex formation. The vanadium complexes exhibited additional absorption bands in the visible region around 389 to 468 nm, which can be attributed to d–d transitions. Their magnetic moment values found in the range of 1.69 &1.72 B.M. which aligns with the presence of a single unpaired electron, confirming a low-spin d^1 configuration and their paramagnetic behaviour. Overall, magnetic data and spectrum changes between the ligands and their metal complexes demonstrate effective coordination and bolster the synthetic compounds' structural stability.

4.2.4. FAB Mass

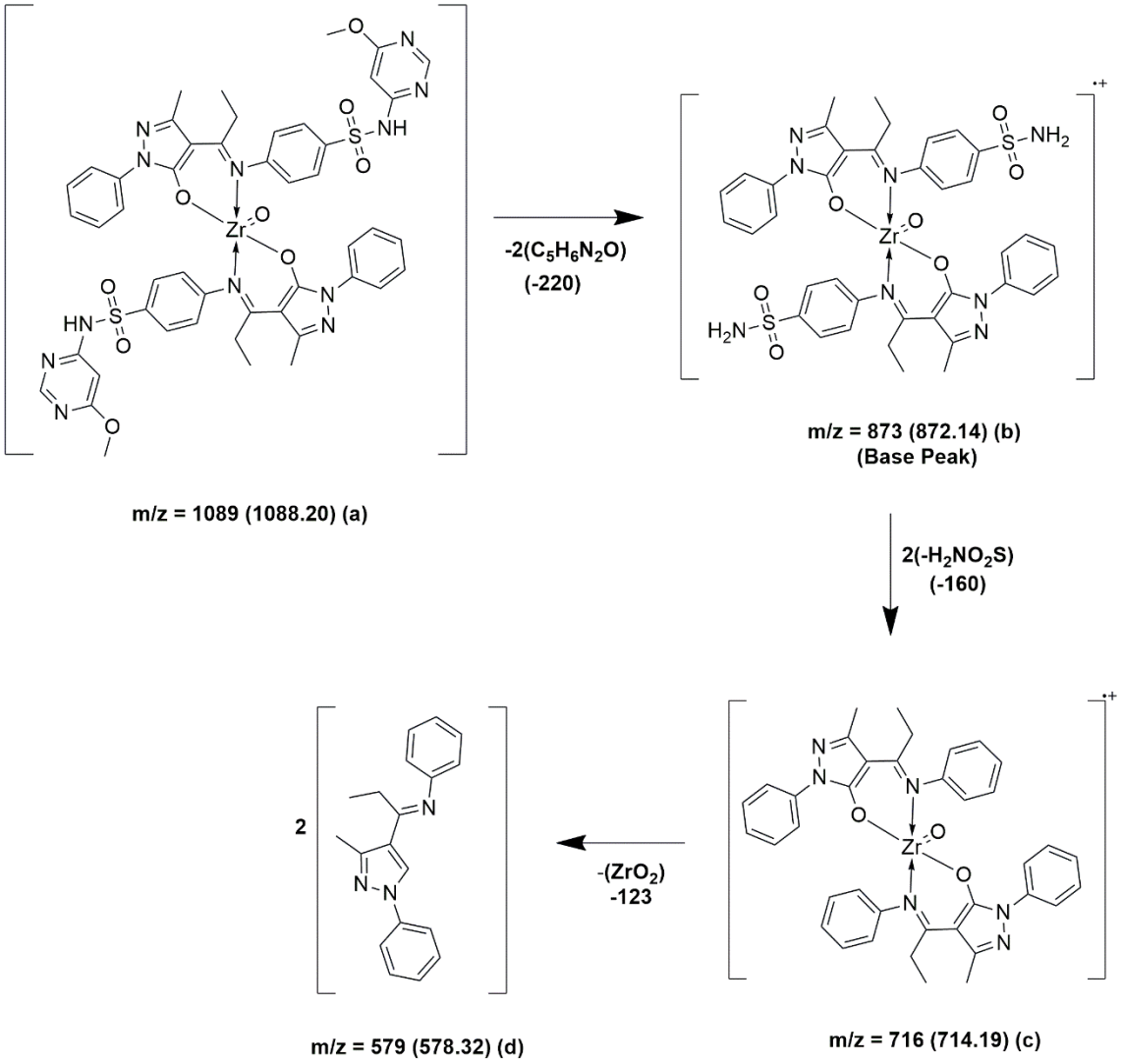

Figure 4.1 Suggested fragmentation pattern of heterochelate $[(L_8)_2ZrO]$

Chapter 5

Computational Analysis, Molecular Docking, Anti-Microbial Activity & Conclusion

5.1. Anti-Microbial and Anti-Fungal Activities

Notably, the complex $[(L_1)_2$ VO] demonstrated the highest antibacterial efficacy compare to reference drug (Streptomycin 24 mm), with a zone of inhibition of 28 mm against *E. coli* and 20 mm against *S. aureus*. Similarly, $[(L_1)_2WO_2]$ also showed considerable activity, exhibiting inhibition zones of 22 mm against *E. coli* and 24 mm against *S. aureus*. These findings indicate a significant enhancement in biological activity upon metal coordination.

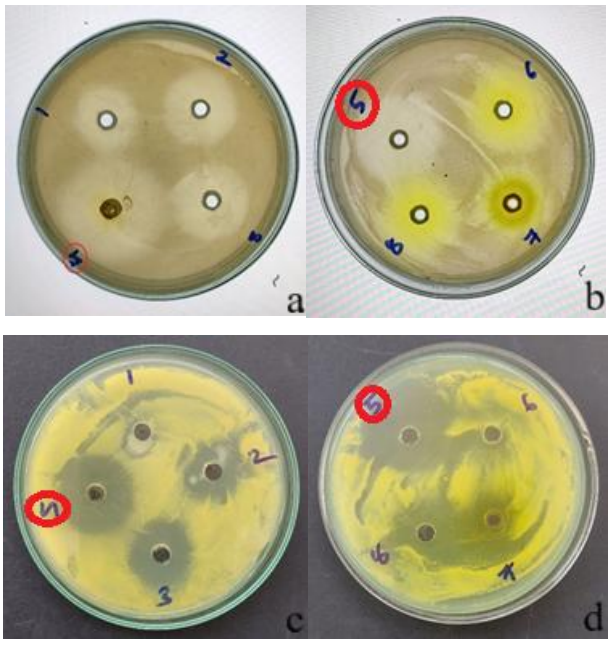

Figure 5.1. Zone of inhibition in mm (a) $[(L_1)_2VO]$ *E. Coli* (b) $[(L_1)_2WO_2]$ *E. Coli* (c) $[(L_1)_2VO]$ *S. aureus* (d) $[(L_1)_2WO_2]$ *S. aureus*

5.2. Computational Analysis of Ligands

The energy gaps (Δ**E**) were calculated using the following equation.

$$\textbf{Energy gap } (\Delta \mathbf{E}) = |\mathbf{E_{HOMO}} - \mathbf{E_{LUMO}}|$$

DFT analysis of ligands L_1–L_9 provided key electronic parameters such as E_{HOMO}, E_{LUMO}, and the energy gap (ΔE). Among the series, L_9 showed the largest ΔE (0.3879 eV), along with the highest E_{HOMO} and lowest E_{LUMO} values, indicating that it is the most stable and least reactive ligand. In contrast, L_4 had the smallest ΔE (0.007 eV), suggesting higher reactivity and a stronger ability to interact with metal centres or biological targets. The differences in ΔE across the ligands highlight variations in their electron-donating and electron-withdrawing tendencies, offering useful insights into their structure activity relationships in coordination chemistry and molecular design.

5.3. Molecular Docking study of Ligands

Molecular docking of ligands L_1–L_9 with the target protein (PDB ID: 1aj0) showed noticeable differences in their binding strengths and interaction patterns. Among all, L_6 demonstrated the strongest binding, with a binding energy of –9.82 kcal/mol and the lowest inhibition constant (63.36 nM). It established two stable hydrogen bonds at 2.22 Å and 2.08 Å distances with ARG63 and GLY191. Ligands L_7 and L_9 also performed well, showing favourable binding energies (–8.30 and –8.79 kcal/mol) and nanomolar inhibition constants. On the other hand, L_4 showed the weakest interaction (–3.92 kcal/mol; 1.33 mM), indicating poor binding affinity. Overall, hydrogen bonding—especially with arginine residues—played a major role in stabilizing the ligand–protein complexes. These results demonstrate how variations in ligand structure and electrical characteristics affect binding effectiveness, with L6 emerging as the most viable option for additional biological research.

5.4. Conclusion

We created new Schiff base ligands from sulfa medication compounds and corresponding heterochelates, and we tested them with mass spectroscopy, IR, UV, and ^{1}H-NMR to ensure their purity and structures. A detailed evaluation of their antifungal and antibacterial properties revealed

significant improvements following metal coordination. DFT investigations revealed that electron-withdrawing substituents have a major impact on HOMO–LUMO energies, providing more information about the electronic behaviour of the ligands. Strong ligand-DHPS binding was further shown by molecular docking, which was reinforced by important hydrophobic, hydrogen-bonding, and π–π stacking interactions that stabilize the complexes. The ligands promise as attractive scaffolds for rational drug design targeting bacterial DHPS is highlighted by their low entropic penalties and structural and electrostatic complementarity. Overall, the findings demonstrate that metal coordination significantly increases antimicrobial effectiveness, especially against Gram-negative bacteria, offering a solid foundation for additional pharmacological and molecular research.

Publications

1. Jani D, Jani D, Paghdar N. Fluorescent Schiff base chelators: A critical review on their sensing abilities for metal ions and cyanide ion. IJBPAS. 2024;13(12):X–X. https://doi.org/10.31032/IJBPAS/2024/13.12.8530
2. Jani DN, Jani DH, Paghdar NA. Rare earth transition metal-based coordination compounds of Schiff base derived from sulpha drug molecules: Synthesis, spectroscopic and in vitro biological screening. Indian Journal of Chemistry. 2025;64:519–527. https://doi.org/10.56042/ijc.v64i5.17525
3. Jani DN, Jani DH, Paghdar NA. Exploring the biological and theoretical aspects of rare earth metal mixed ligand complexes: A synergistic approach. Research Journal of Chemistry and Environment. 2025;29(10):54–60. https://doi.org/10.25303/2910rjce05406

Reference

[1] A. Hamad, et al., "Development of sulfonamide-based Schiff bases targeting urease inhibition: Synthesis, characterization, inhibitory activity assessment, molecular docking and ADME studies," *Bioorganic Chemistry*, vol. 102, pp. 104057, 2020.

[2] M. Pervaiz, A. Munir, A. Riaz, Z. Saeed, U. Younas, M. Imran, S. Ullah, R. Bashir, A. Rashid, and A. Adnan, "Inorganic Chemistry Communications," *Inorganic Chemistry Communications*, vol. 141, pp. 109459, 2022.

[3] H. H. Amer, E. H. Eldrehmy, S. M. Abdel-Hafez, Y. S. Alghamdi, M. Y. Hassan, and S. H. Alotaibi, "Scientific reports," *Scientific Reports*, vol. 11, no. 1, pp. 17953, 2021.

[4] S. Mondal, T. K. Mondal, Y. Rajesh, M. Mandal, and C. Sinha, "Polyhedron," *Polyhedron*, vol. 151, pp. 344–354, 2018.

[5] A. M. Ramadan, H. A. Bayoumi, and R. M. I. Elsamra, "Applied Organometallic Chemistry," *Applied Organometallic Chemistry*, vol. 35, no. 12, pp. e6412, 2021.

[6] N. A. Danilkina, A. A. Vasileva, and I. A. Balova, "Russian Chemical Reviews," *Russian Chemical Reviews*, vol. 89, no. 1, pp. 125, 2020.

[7] M. S. Masoud, A. A. Soayed, S. A. Almesmari, and R. M. I. Elsamra, "Journal of Inorganic and Organometallic Polymers and Materials," *Journal of Inorganic and Organometallic Polymers and Materials*, vol. 31, pp. 2842–2858, 2021.

[8] V. Ambike, S. Adsule, F. Ahmed, Z. Wang, Z. Afrasiabi, E. Sinn, F. Sarkar, and S. Padhye, "Copper conjugates of nimesulide Schiff bases targeting VEGF, COX and Bcl-2 in pancreatic cancer cells," *Journal of Inorganic Biochemistry*, vol. 101, no. 10, pp. 1517–1524, 2007.

[9] S. Arulmurugan, H. P. Kavitha, and B. R. Venkatraman, "Biological activities of Schiff base and its complexes: a review," *Rasayan Journal of Chemistry*, vol. 3, no. 3, pp. 385–410, 2010.

[10] A. Hameed, M. Al-Rashida, M. Uroos, S. A. Abid Ali, and K. M. Khan, "Schiff bases in medicinal chemistry: a patent review (2010–2015)," *Expert Opinion on Therapeutic Patents*, vol. 27, no. 1, pp. 63–79, 2017.

[11] K. D. Mjos and C. Orvig, "Metallodrugs in medicinal inorganic chemistry," *Chemical Reviews*, vol. 114, no. 8, pp. 4540–4563, 2014.

[12] P. Gajera, M. Vadodaria, and R. Parmar, "Transition metal-based coordination compounds of Schiff base derived from drug molecules: Synthesis, spectroscopic and in vitro biological screening," *[Journal name not provided]*, 2024.

[13] P. Rathi, D. P. Singh, and P. Surain, "Synthesis, characterization, powder XRD and antimicrobial-antioxidant activity evaluation of trivalent transition metal macrocyclic complexes," *Comptes Rendus Chimie*, vol. 18, no. 4, pp. 430–437, 2015.

[14] M. F. M. Ribeiro, et al., "Voltammetric determination of cocaine using carbon screen-printed electrodes chemically modified with uranyl Schiff base films," *Electroanalysis*, vol. 28, no. 2, pp. 320–326, 2016.

[15] B. S. Creaven, et al., "Anticancer and antifungal activity of copper(II) complexes of quinolin-2(1H)-one-derived Schiff bases," *Inorganica Chimica Acta*, vol. 363, no. 14, pp. 4048–4058, 2010.

[16] E. Keshavarzian, et al., "Heterodinuclear Cu–Gd (3d–4f) complex with di-compartmental Schiff base ligand in biological activity: Synthesis, crystal structure, catecholase activity and DNA & BSA-binding studies," *Journal of Molecular Liquids*, vol. 345, pp. 117785, 2022.

[17] D. H. Jani and C. K. Modi, "Mn(III) mixed-ligand complexes with bis-pyrazolones and ciprofloxacin drug: synthesis, characterization and antibacterial activities," *Applied Organometallic Chemistry*, vol. 25, no. 6, pp. 429–436, 2011.

[18] D. H. Jani, H. Keharia, C. K. Modi, and H. S. Patel, "Novel drug-based Fe(III) heterochelates: synthetic, spectroscopic, thermal and in-vitro antibacterial significance," *Applied Organometallic Chemistry*, vol. 24, no. 2, pp. 99–111, 2010.